

Trapping of an electromagnetic wave by the boundary of a time-varying plasma

M. I. Bakunov*

Department of Radiophysics, University of Nizhny Novgorod, Nizhny Novgorod, Russia

A. V. Maslov

Department of Physics, Washington State University, Pullman, Washington 99164-2814

(Received 3 July 1997)

The interaction of an electromagnetic wave with a plasma half-space whose density instantaneously grows in time due to ionization processes is considered. Unlike previous works in this field treating the degenerate case of normal incidence, oblique incidence of a TM polarized wave on the plasma boundary is investigated. A distinguishing feature of the case of oblique incidence is the creation of two frequency downshifted surface waves propagating along the plasma boundary in the opposite directions. Their frequency shifts and amplitudes as well as characteristics of the other steady-state modes are examined. Angular and frequency distributions of outgoing transient radiation are discussed. In particular, we have shown that the frequency upshift of the generated transients can be higher than for the normal incidence case reported earlier. The results are presented for both gaseous and solid-state plasma. [S1063-651X(98)12705-8]

PACS number(s): 52.40.Db, 52.35.-g, 84.40.Az

I. INTRODUCTION

The study of the interaction between electromagnetic waves and spatially bounded plasmas whose density is rapidly growing is of considerable interest due to its potential applications in generation of tunable microwave radiation. Fante [1] was the first who discussed some peculiarities of the reflection of electromagnetic signals from the plane boundary of a time-varying plasma. Later, Kalluri [2] presented a more complete analysis including both steady-state solution and transient processes for the case of the reflection of a time-harmonic electromagnetic wave by a suddenly created (switched) plasma half-space. Kalluri and Goteti [3] brought the solved problem closer to practical situations by considering a switched plasma slab. Finally, the effects of a magnetized plasma were examined by Kalluri [4].

In all of the above papers, however, only the degenerate case of normal incidence of an electromagnetic wave on the boundary of a time-varying plasma was treated. In this paper, we examine oblique incidence of a TM polarized wave on the boundary of a plasma half-space whose density instantaneously grows in time from one value to another. A distinguishing feature of the case of oblique incidence, which is inherent only in TM polarization of the incident wave, is the possibility of the creation of surface waves guided by the plasma boundary. In other words, a part of the original wave energy may be trapped by the boundary of the time-varying plasma via transformation into surface waves. The phenomenon of trapping was earlier demonstrated by Bakunov and Zaitsev [5] in the special case in which the initial plane wave travels in free space and the boundary of the switched plasma half-space is perpendicular to the wave front.

A solution to the problem is developed using Laplace transforms and methods of contour integration in the complex plane. It is shown that two frequency downshifted sur-

face waves propagating along the plasma boundary in the opposite directions are excited by the temporal discontinuity of the medium. The absolute values of their frequencies are equal, the signs are opposite. We study the dependence of the surface wave frequencies on the angle of incidence of the input wave and the final plasma density. The surface wave amplitudes are calculated and analyzed as well. A free-streaming mode consisting of static magnetic field and corresponding spatial distribution of electric current is shown to be excited in the plasma half-space. It has a more complicated character compared with the cases considered in Refs. [6–9]. We also investigate the angular distribution of the frequency and energy of transient outgoing radiation both in vacuum and in the plasma. The results are found to differ considerably for two cases: when total reflection of the incident wave by the plasma half-space occurs and when it is absent.

Concerning applications, our consideration is oriented to microwave and (sub)millimeter wave interactions with both nonstationary gaseous plasmas, being widely used in modern experiments on frequency shifting [6–13], and, to a more significant extent, solid-state (semiconductor) plasmas whose densities fast temporal growth may be provided via photoionization by laser light [14,15]. It is well known that surface modes of an open waveguiding structure (including the plasma-vacuum boundary as the simplest one) do not couple directly to the incident bulk radiation because of the impossibility to satisfy simultaneously two conservation laws—namely, those of energy (wave frequency) and in-plane momentum (wave vector) [16,17]. Thus, certain techniques based on the creation of space inhomogeneities such as profiled or rough surfaces and diaphragms or by providing the spatial synchronization of the modes by applying the method of attenuated total internal reflection are used for coupling the electromagnetic radiation into open waveguiding structures [16,17]. Another possible scheme for coupling incident radiation to surface waves is via nonlinear techniques [18]. The phenomenon of trapping presented in this paper pro-

*Electronic address: bakunov@rf.unn.runnet.ru

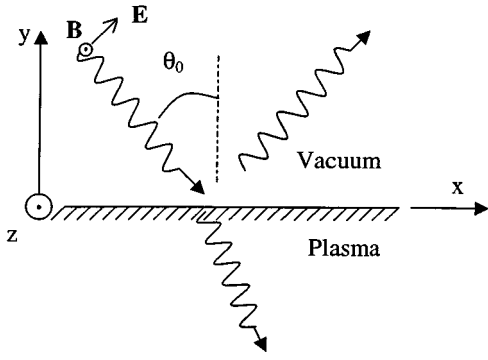


FIG. 1. Geometry of the problem.

vides us with a fundamentally different technique exploiting an inhomogeneity in time (nonstationarity) of the waveguiding medium to frequency synchronize guided modes. On physical grounds one can envision this coupling mechanism in the following manner. By using the nonstationarity of the dielectric constant of the waveguiding medium controlled by laser pulses we create transient fields, which in turn can generate the frequency downshifted guided waves. Some preliminary results of the work have been briefly reported in Ref. [19].

The paper is organized as follows. In Sec. II we introduce our model and derive basic equations as well as initial conditions for the fields. In Sec. III we apply a Laplace transform technique in order to solve Maxwell's equations. Then we calculate the Laplace transform for the magnetic field and discuss general properties of the solution. In Sec. IV we focus on the characteristics of the excited steady-state modes such as surface waves, the dc current with corresponding dc magnetic field, and bulk waves. Transient fields are calculated in Sec. V. Section VI gives our conclusion.

II. FORMULATION OF THE PROBLEM AND BASIC EQUATIONS

Initially, when $t < 0$, a plane TM polarized electromagnetic wave of frequency ω_0 is incident at an arbitrary angle θ_0 from vacuum ($y > 0$) on a lossless plasma half-space ($y < 0$) with free electron density N_1 (see Fig. 1). The magnetic field of the incident wave has only one component, which is given by

$$B_z(x, y, t) = B_0 e^{i\omega_0 t - ih_0 x + ig_0 y}, \quad (1)$$

with $h_0 = (\omega_0/c) \sin \theta_0$ and $g_0 = (\omega_0/c) \cos \theta_0$ the tangential and normal components of the wave vector, respectively. This wave gives rise to the reflected wave in vacuum and transmitted wave in the plasma, which are defined by the reflection coefficient $R = T - 1$ and transmission coefficient (relative to the magnetic field) [20]

$$T = \frac{2g_0}{g_0 + g_1/\epsilon_1}, \quad (2)$$

where $g_1 = (\omega_0/c) \sqrt{\epsilon_1 - \sin^2 \theta_0}$ is the normal component of the wave vector in the plasma, $\epsilon_1 = \epsilon_b (1 - \omega_{p1}^2/\omega_0^2)$ is the dielectric constant of the plasma, ϵ_b is the background dielectric constant in the case of a semiconductor plasma (ϵ_b

= 1 for a gaseous plasma), and $\omega_{p1} = \sqrt{4\pi e^2 N_1/m\epsilon_b}$ is the plasma frequency; e and m are the charge and mass (effective) of electrons in the plasma, respectively. In the case of total internal reflection ($\epsilon_1 < \sin^2 \theta_0$) the imaginary part of g_1 is chosen to be negative as dictated by causality.

Then, at $t = 0$, the free electron density grows instantly (i.e., the rise time of the plasma is much shorter than ω_0^{-1}) from N_1 to N_2 due to effect of an external ionizing factor. The evolution of the wave fields in time is governed by Maxwell's equations

$$\frac{\partial E_x}{\partial y} + ih_0 E_y = \frac{1}{c} \frac{\partial B_z}{\partial t}, \quad (3a)$$

$$\frac{\partial B_z}{\partial y} = \frac{1 + (\epsilon_b - 1)\Theta(-y)}{c} \frac{\partial E_x}{\partial t} - \frac{4\pi e}{c} \Theta(-y) \times [N_1 V_{1x} + \Theta(t) \Delta N V_{2x}], \quad (3b)$$

$$ih_0 B_z = \frac{1 + (\epsilon_b - 1)\Theta(-y)}{c} \frac{\partial E_y}{\partial t} - \frac{4\pi e}{c} \Theta(-y) \times [N_1 V_{1y} + \Theta(t) \Delta N V_{2y}]. \quad (3c)$$

The equation for electron motion is

$$\frac{\partial \mathbf{V}_{1,2}}{\partial t} = -\frac{e}{m} \mathbf{E}, \quad (4)$$

where $\Theta(\xi)$ is the unit step function, $\Delta N = N_2 - N_1$ is the temporal plasma density discontinuity, and $\mathbf{V}_{1,2}$ are the velocities of the background electrons (i.e., those in the plasma for $t < 0$) and the newly created ones (at $t = 0$), respectively. In Eqs. (3) we have taken into account the conservation of momentum $\exp(-ih_0 x)$ in the (x, z) plane, which follows from the two-dimensional translational invariance of the system. The newly created electrons are assumed to be born with zero velocity [22], i.e.,

$$\mathbf{V}_2(x, y, 0^+) = \mathbf{0}, \quad (5)$$

and are set in motion only for $t > 0$.

Equations (3) and (4) with condition (5) form a closed system of equations which is valid for $-\infty < t < +\infty$. With Laplace transform in mind let us find the values of E_x , E_y , B_z , and \mathbf{V}_1 at $t = 0^+$. They can be easily obtained by integration of Eqs. (3) and (4) over the vanishing density growth time (i.e., from $t = 0^-$ to 0^+). This yields the continuity of E_x , E_y , B_z , and \mathbf{V}_1 over the temporal discontinuity. Thus, for the initial conditions for E_x, E_y, B_z in the Laplace transforms, we should take their values at $t = 0^-$ corresponding to the standard pattern of the reflection and transmission of the incident wave on the boundary of a semi-infinite medium with the dielectric constant ϵ_1 (e.g., see [20]). In addition, for velocity of the background electrons for $t < 0$, according to Eq. (4), we write

$$\mathbf{V}_1(x, y, 0) = -\frac{e}{im\omega_0} \mathbf{E}(x, y, 0). \quad (6)$$

III. LAPLACE TRANSFORMS

Applying Laplace transformation to Eqs. (3) and (4) and eliminating the Laplace transforms of the components of the electric field and electrons' velocities, we arrive at the following equation for the Laplace transform of the magnetic field ($\mathcal{L}[B_z(x,y,t)] = b(x,y,s)$, s is Laplace variable):

$$\varepsilon_2 \frac{\partial}{\partial y} \left(\frac{1}{\varepsilon_2} \frac{\partial b}{\partial y} \right) - \frac{1}{c^2} (s^2 \varepsilon_2 + c^2 h_0^2) b = F(x,y,s), \quad (7)$$

with the function $F(x,y,s)$ acting like a spatially distributed source:

$$F(x,y,s) = -\frac{1}{c^2} (s \varepsilon_2 + i \omega_0 \gamma) B_z(x,y,0) - E_x(x,y,0) \frac{\varepsilon_2}{c} \frac{\partial}{\partial y} \left(\frac{\gamma}{\varepsilon_2} \right). \quad (8)$$

Here $\varepsilon_2(y,s)$ and $\gamma(y,s)$ are equal to unity in vacuum and $1 + \omega_{p2}^2/s^2$ and $1 - \omega_{p1}^2/is\omega_0$ in the plasma, respectively; $\omega_{p2} = \sqrt{4\pi e^2 N_2/m\varepsilon_b}$ is the plasma frequency for $t > 0$.

Solutions of Eq. (7) in the homogeneous regions $y > 0$ and $y < 0$ may be easily obtained:

$$b(x,y,s) = \begin{cases} \frac{B_z(x,y,0)}{s - i\omega_0} + A_v(s) e^{-ih_0x - \kappa_v y}, & \text{if } y > 0 \\ \frac{s(s + i\omega_0) + \Delta\omega_p^2}{s(s^2 + \omega_0^2 + \Delta\omega_p^2)} B_z(x,y,0) + A_p(s) e^{-ih_0x + \kappa_p y}, & \text{if } y < 0, \end{cases} \quad (9)$$

where $\kappa_p = \sqrt{s^2 \varepsilon_2/c^2 + h_0^2}$ and $\kappa_v = \sqrt{s^2/c^2 + h_0^2}$, their real parts being taken positive to satisfy the radiation condition; $\Delta\omega_p^2 = \omega_{p2}^2 - \omega_{p1}^2$. The quantities A_v and A_p in Eq. (9) can be determined by matching the solutions (9) at the $y=0$ by the boundary conditions

$$\{b\} = 0, \quad \left\{ \frac{1}{\varepsilon_2} \frac{\partial b}{\partial y} + \frac{\gamma}{c\varepsilon_2} E_x(x,y,0) \right\} = 0, \quad (10)$$

which result from integration of Eq. (7) across the spatial discontinuity at $y=0$; curly brackets denote the difference of the enclosed expressions over the interface. Evidently, the second condition in Eq. (10) is equivalent to the continuity of the tangential component of the electric field transform. Substitution of Eq. (9) into (10) gives the following expressions for A_v and A_p :

$$A_v(s) = B_0 T \frac{s \Delta\omega_p^2 (s^2 \varepsilon_2 g_1 - i \omega_0^2 \varepsilon_1 \kappa_p)}{(s - i\omega_0)(s^2 + \omega_0^2 + \Delta\omega_p^2) \omega_0 \varepsilon_1 D(s)}, \quad (11a)$$

$$A_p(s) = B_0 T \frac{\varepsilon_b \Delta\omega_p^2 (s^2 + \omega_{p2}^2) (s^2 g_1 + i \omega_0^2 \varepsilon_1 \kappa_v)}{s(s - i\omega_0)(s^2 + \omega_0^2 + \Delta\omega_p^2) \omega_0 \varepsilon_1 D(s)}, \quad (11b)$$

where

$$D(s) = s^2 (\kappa_p + \varepsilon_2 \kappa_v). \quad (12)$$

The first terms in Eq. (9) are forced responses and the corresponding inverse Laplace transforms contribute to $B_z(x,y,t)$ immediately after the density growth beginning at $t=0^+$. In vacuum ($y > 0$) this contribution is equal to the incident wave (1) and the reflected wave with the reflection coefficient $R = T - 1$ [see Eq. (2)]. In the plasma ($y < 0$) the forced response differs from the initially transmitted wave and has the following form:

$$B_z(x,y,t) = B_z(x,y,0) \left(\frac{\Delta\omega_p^2}{\omega_0^2 + \Delta\omega_p^2} + \sum_{\pm} \frac{\omega_0}{2} \frac{\omega_0 \pm \sqrt{\omega_0^2 + \Delta\omega_p^2}}{\omega_0^2 + \Delta\omega_p^2} e^{\pm it \sqrt{\omega_0^2 + \Delta\omega_p^2}} \right). \quad (13)$$

The general expression (13) reduces to the more particular results derived earlier for the case of a suddenly created homogeneous plasma [6,7]. Increased generality of Eq. (13) is connected with the initial preionization of the medium and the more complicated y dependence provided by $B_z(x,y,0) = TB_0 \exp(ig_1 y - ih_0 x)$ corresponding to the oblique incidence of the original wave; this is important especially in the case

of total internal reflection. The time-independent term in Eq. (13) describes the static magnetic field caused by the constant component of the velocity of both the background and newly created electrons. This component is acquired through the driving of the electrons beginning at $t=0$ by the waves of frequencies $\pm \sqrt{\omega_0^2 + \Delta\omega_p^2}$ appearing in Eq. (13). This may be easily shown by solving Eq. (4) with the latter waves as a

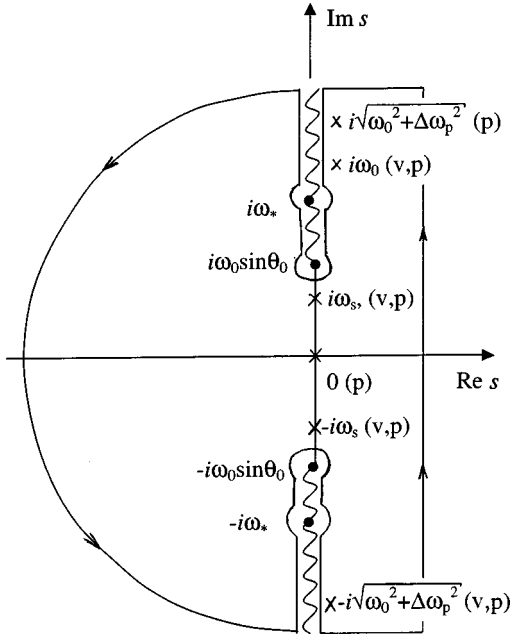


FIG. 2. Diagram of the closed path for contour integration in the s plane at $t > y/c$ ($y > 0$) and $t > |y|\sqrt{\epsilon_b}/c$ ($y < 0$). The correspondence of the poles (marked by crosses) to the functions A_v and A_p is shown in brackets. In vacuum the pole $s = -i\sqrt{\omega_0^2 + \Delta\omega_p^2}$ exists only if $\sqrt{\omega_0^2 + \Delta\omega_p^2} > \omega_*$, i.e., $\epsilon_1 > \sin^2 \theta_0$.

force and initial conditions (5) and (6). Such a static type of solution is common for problems involving nonstationary plasma and often called the free-streaming mode [9,21]. The terms of frequencies $\pm\sqrt{\omega_0^2 + \Delta\omega_p^2}$ in Eq. (13) arise due to the transmission and reflection of the initial wave within the plasma half-space on the temporal discontinuity as in the case of normal incidence [2–4]. When the original wave penetrates at $t < 0$ into the plasma the wave of frequency $\sqrt{\omega_0^2 + \Delta\omega_p^2}$ travels from the boundary $y=0$ to $y=-\infty$; the wave of frequency $-\sqrt{\omega_0^2 + \Delta\omega_p^2}$ comes from $y=-\infty$ and travels towards the boundary. In the case of total reflection of the original wave at $t < 0$, these forced waves decay in the plasma like the original wave.

The second terms in Eq. (9) are free-wave types of solutions. The values of the inverse Laplace transform of these terms vanish for $t < y/c$ in vacuum and for $t < |y|\sqrt{\epsilon_b}/c$ in the plasma because of the presence of $\exp(\mp\kappa_{v,p}y + st)$ in the integrands of the inversion integrals (the integration path in this case should be closed on the right half-plane of the complex variable s). For $t > y/c$ (if $y > 0$) and for $t > |y|\sqrt{\epsilon_b}/c$ (if $y < 0$) the integration path should be closed on the left half-plane thereby switching on the free-wave contribution. Thus, the region of the transient processes starts to move from the boundary $y=0$ beginning at the moment $t=0$ into both vacuum (with the light velocity c) and the plasma (with the velocity $c/\sqrt{\epsilon_b}$).

For the evaluation of the steady-state solutions and angular distribution of outgoing transient radiation, the closed integration path in the inverse Laplace transform of the second terms in Eq. (9) is chosen appropriately as shown in Fig. 2. The integration path lies in the Riemann sheet of the complex

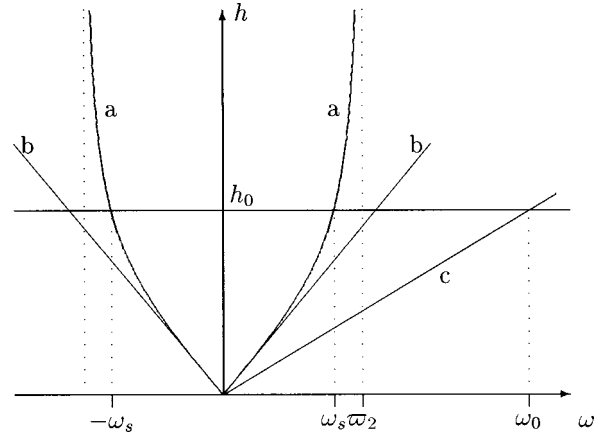


FIG. 3. Kinematic diagram: in-plane wave vector h vs frequency ω . Curves labeled a : Branches of the dispersion curve for the surface waves at the boundary of a plasma half-space with density N_2 ; b : light lines $h = \pm\omega/c$; c : line $h = (\omega/c)\sin\theta_0$. Two intersections of the surface wave dispersion curve with the line $h = h_0$ give frequencies $\pm\omega_s$ for the excited surface waves.

s plane where the real parts of κ_v and κ_p are positive to ensure evanescence of the fields at $y = \pm\infty$. The branch cuts (due to the double-valued functions κ_v and κ_p) run along the imaginary axis from the branch points $\pm i\omega_0 \sin\theta_0$ and $\pm i\omega^*$ [$\omega^* = \sqrt{\omega_p^2 + \omega_0^2(\sin^2\theta_0)/\epsilon_b}$] to infinity (for definiteness $\omega^* > \omega_0 \sin\theta_0$ in Fig. 2). The residues of $A_v(s)$ and $A_p(s)$ as well as the forced responses (1) and (13) contribute to the steady-state solution. The integration over the branch cuts represents transient processes including outgoing radiation. In Fig. 2 the poles $s = i\omega_0$ and $s = \pm i\sqrt{\omega_0^2 + \Delta\omega_p^2}$ are shown on the right sides of the branch cuts as it follows from the physically evident requirement that corresponding waves should travel away from the boundary. It is easy to show that the forced response of frequency $+\sqrt{\omega_0^2 + \Delta\omega_p^2}$ in Eq. (13) is canceled by the residue of $A_p(s)$ at the pole $s = i\sqrt{\omega_0^2 + \Delta\omega_p^2}$ for $t > |y|\sqrt{\epsilon_b}/c$. The forced response of frequency $-\sqrt{\omega_0^2 + \Delta\omega_p^2}$ in Eq. (13) is canceled by the residue of $A_p(s)$ at the pole $s = -i\sqrt{\omega_0^2 + \Delta\omega_p^2}$ for $t > |y|\sqrt{\epsilon_b}/c$ only if $\sqrt{\omega_0^2 + \Delta\omega_p^2} < \omega_*$, i.e., $\epsilon_1 < \sin^2\theta_0$ (initial field in the plasma is evanescent). In vacuum the pole $s = -i\sqrt{\omega_0^2 + \Delta\omega_p^2}$ exists only in the case when $\sqrt{\omega_0^2 + \Delta\omega_p^2} > \omega_*$, i.e., $\epsilon_1 > \sin^2\theta_0$.

IV. STEADY-STATE SOLUTION

Here we consider the steady-state solution represented by a number of modes both in vacuum and in the plasma.

A. Surface waves

A characteristic feature of the case of oblique incidence of the original wave on the boundary of a nonstationary plasma is the excitation of surface waves guided by the plasma boundary. These waves are described by the residues of $A_v(s)$ and $A_p(s)$ at the points where Eq. (12) for $D(s)$ equals zero. The equation $D(s) = 0$ has two roots $s = \pm i\omega_s$ where

$$\omega_s = \sqrt{\frac{1 + \varepsilon_b}{2\varepsilon_b}} \sqrt{\varpi_2^2 + \omega_0^2 \sin^2 \theta_0} - \sqrt{\varpi_2^4 + \omega_0^4 \sin^4 \theta_0 - 2\varpi_2^2 \omega_0^2 \sin^2 \theta_0} \frac{\varepsilon_b - 1}{\varepsilon_b + 1}, \quad (14)$$

with $\varpi_2 = \omega_{p2} / \sqrt{1 + \varepsilon_b^{-1}}$ the limiting frequency for the surface waves [23].

Therefore, two surface waves are excited as a result of the plasma density growth. One of the waves (of frequency $\omega_s > 0$) propagates in the positive x direction, the other one (of frequency $-\omega_s < 0$) in the negative x direction. This result may be illustrated by a kinematic diagram (see Fig. 3). The frequencies of the surface waves correspond to intersection points of the horizontal line $h = h_0$, which represents the invariance of the spatial structure of the wave fields in the interface $y = 0$ on the temporal discontinuity, and two branches (for $\omega > 0$ and for $\omega < 0$) of the dispersion curve for the surface waves guided by the plasma half-space with free electron density N_2 [23]

$$h = \sqrt{\frac{\omega^2}{c^2} \frac{1 - \omega^2/\omega_{p2}^2}{1 - \omega^2/\varpi_2^2}}. \quad (15)$$

It is evident from Fig. 3 that the excited surface waves are frequency down shifted ($\omega_s < \omega_0$). The frequency conversion coefficient ω_s/ω_0 increases with the final (for $t > 0$) plasma density N_2 and tends to the limit $\omega_s/\omega_0 \rightarrow \sin \theta_0$ when $N_2 \rightarrow \infty$. In this limit the velocity of the surface waves approaches *in vacuo* speed of light and the waves themselves lose their localization and degenerate into plane waves traveling in vacuum along the perfectly conducting half-space $y < 0$.

Figure 4 shows the frequency conversion coefficient ω_s/ω_0 versus the parameter ϖ_2/ω_0 , which characterizes the final plasma density, for different values of the incident angle θ_0 and the background dielectric constant ε_b . The interval of possible values of the frequency conversion coefficient is bounded from above by the line segments $\omega_s = \varpi_2$ and $\omega_s/\omega_0 = 1$, which corresponds to the limit $\varepsilon_b \rightarrow \infty$, $\theta_0 \rightarrow \pi/2$ in Eq. (14).

As we see from Fig. 4, an increase in ε_b for a fixed θ_0 causes a more rapid increase in the frequency conversion coefficient ω_s/ω_0 with ϖ_2/ω_0 . In the case $\varepsilon_b \gg 1$, which is usual for typically used semiconductors where $\varepsilon_b \sim 10 - 20$ [24], Eq. (14) reduces to a simple approximation

$$\omega_s \approx \min\{\varpi_2, \omega_0 \sin \theta_0\}. \quad (16)$$

The result (16) becomes evident if we take into account that for $\varepsilon_b \gg 1$ the limiting frequency is close to the plasma frequency ($\varpi_2 \approx \omega_{p2}$) and, consequently, as follows from Eq. (15), the dispersion curve branches approach the broken lines consisting of the light-line segments in the interval $-\varpi_2 < \omega < \varpi_2$ and then continue upward at $\omega = \pm \varpi_2$. Formula (16) means that for $\varepsilon_b \gg 1$ the frequency conversion coefficient plotted as a function of the parameter ϖ_2/ω_0 is close to the asymptotic line $\omega_s = \varpi_2$ until ϖ_2/ω_0 becomes equal to $\sin \theta_0$, and after that remains constant.

The surface wave amplitudes (magnitude of the magnetic field at the boundary) are determined by the residues of $A_v(s)$ and $A_p(s)$ at the poles $s = \pm i\omega_s$ and can be written as

$$B_{\pm} = B_0 T \frac{\Delta \omega_p^2 \omega_0 \sin^2 \theta_0 (\omega_{p2}^2 - \omega_s^2) \sqrt{\omega_0^2 \sin^2 \theta_0 - \omega_s^2} (\omega_0^2 \sqrt{\omega_0^2 \sin^2 \theta_0 - \omega_s^2} + i \omega_s^2 c g_1 / \varepsilon_1)}{(\omega_0 \mp \omega_s) (\omega_0^2 - \omega_s^2 + \Delta \omega_p^2) (2\omega_0^2 \sin^2 \theta_0 - \omega_s^2) (\omega_{p2}^2 \omega_0^2 \sin^2 \theta_0 - \omega_s^4)}. \quad (17)$$

As one can see from Eq. (17), the amplitude of the backward wave is always less than of the forward one: $B_-/B_+ = (\omega_0 - \omega_s)/(\omega_0 + \omega_s) < 1$. Both amplitudes B_{\pm} vanish at $\theta_0 = 0$, i.e., for normal incidence of the original wave on the boundary. For grazing incidence $\theta_0 = 90^\circ$ and if $\varepsilon_1 \neq 1$ the amplitudes B_{\pm} vanish as well since the incident wave does not penetrate into the plasma ($T = 0$) and the fields are not affected by the density shift in the plasma. However, if $\varepsilon_1 = 1$, i.e., the plasma is created in a gas at $t = 0$, the surface waves will have finite amplitudes for $\theta = 90^\circ$ (see [5]).

Figure 5 shows the amplitude coefficient $|B_+|/B_0$ for the forward surface wave as a function of the angle of incidence θ_0 of the original wave and the plasma density shift $\Delta N/N_c$ [$N_c = m \omega_0^2 \varepsilon_b / (4\pi e^2)$ is the critical plasma density for the original wave, $\Delta N/N_c = \Delta \omega_p^2 / \omega_0^2$] in the simple case when the original wave propagates initially in free-space (practically in a gas $\varepsilon_1 \approx 1$) and a plasma half-space $y < 0$ is sud-

denly created at $t = 0$. For this case $\omega_{p1} = 0$, $\varepsilon_b = 1$ are taken in Eqs. (14) and (17). As we see from Fig. 5, the maximum value of the amplitude coefficient $|B_+|/B_0$ is achieved at $\theta_0 = 90^\circ$, i.e., when the boundary of the suddenly created gaseous plasma half-space is perpendicular to the original wave front, and decreases monotonically with decreasing θ_0 vanishing at $\theta_0 = 0$, i.e., for normal incidence treated in [2]. The amplitude approaches the maximum value $|B_+|/B_0 = 2$ at $\theta_0 = 90^\circ$ and $\Delta N/N_c \rightarrow \infty$ as in Ref. [5].

Figure 6 shows the coefficient $|B_+|/B_0$ for the forward surface wave as a function of the angle of incidence θ_0 and the plasma density shift $\Delta N/N_c$ for $\varepsilon_b = 10$ (semiconductor plasma) and $\varepsilon_1 = 0.8$ ($\omega_{p1}/\omega_0 \approx 0.96$). A distinguishing feature of the plot is a break of its surface which corresponds to the angle of total internal reflection of the original wave $\tilde{\theta}_0 \approx 62^\circ$ ($\sin \tilde{\theta}_0 = \sqrt{\varepsilon_1}$). As we see from Fig. 6, the most favorable conditions for the excitation of the forward surface

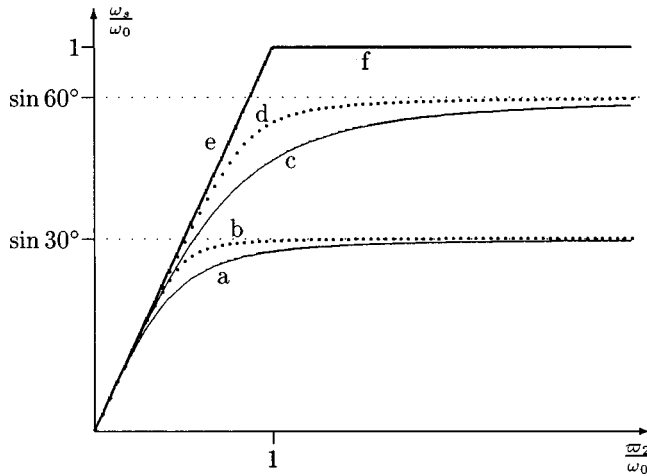


FIG. 4. Frequency conversion coefficient ω_s/ω_0 vs the parameter ω_2/ω_0 for *a*: $\theta_0=30^\circ$ and $\varepsilon_b=1$; *b*: $\theta_0=30^\circ$ and $\varepsilon_b=10$; *c*: $\theta_0=60^\circ$ and $\varepsilon_b=1$; *d*: $\theta_0=60^\circ$ and $\varepsilon_b=10$. Possible values of ω_s/ω_0 are bounded from above by the line segments $\omega_s=\omega_2$ (*e*) and $\omega_s/\omega_0=1$ (*f*).

wave are relatively small density shifts $\Delta N/N_c \sim 2$ ($\Delta N/N_1 \approx \Delta N/N_c$ for $\omega_{p1}/\omega_0 \approx 0.96$); the possibility of fast significant growth of the free-carrier density in semiconductors via photoionization is intensively discussed in the literature, e.g., see Ref. [14]). For these values of the density shift the amplitude of the surface wave is a smooth function of the incident angle θ_0 and reaches the maximum at $\theta_0 \approx 80^\circ$, i.e., rather far from grazing incidence. The interval of significant values of $|B_+|/B_0$ narrows rapidly with increase of $\Delta N/N_c$ and moves very close to grazing incidence $\theta_0=90^\circ$. This makes it practically impossible to attain efficient transformation of the original wave energy into the surface modes for large density shifts. Moreover, at high density shifts $\Delta N/N_c \rightarrow \infty$ the amplitude behaves like

$$B_+ \approx B_0 \frac{4i(\pi/2 - \theta_0)\delta}{(\pi/2 - \theta_0)^2 + \delta^2}, \quad (18)$$

with the small parameter $\delta = \omega_0/\sqrt{\varepsilon_b}\omega_{p2}$. According to Eq. (18) the amplitude $|B_+|/B_0$ exhibits a narrow peak of width $\sim \delta$ with the maximum value $|B_+|/B_0=2$ reached at $\theta_0 \approx \pi/2 - \delta$. The smaller δ the narrower and closer to θ_0

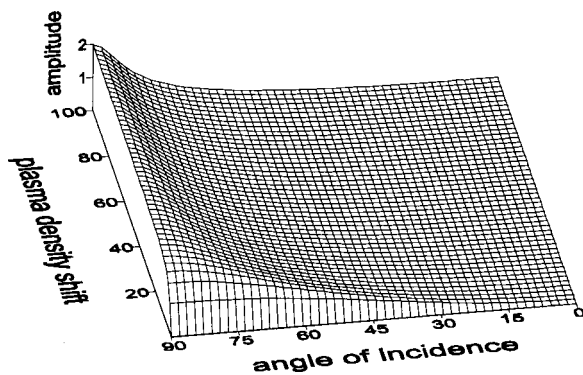


FIG. 5. Amplitude of the forward wave $|B_+|/B_0$ vs the original wave angle of incidence θ_0 and plasma density shift $\Delta N/N_c$ for the special case when $N_1=0$ and $\varepsilon_b=1$.

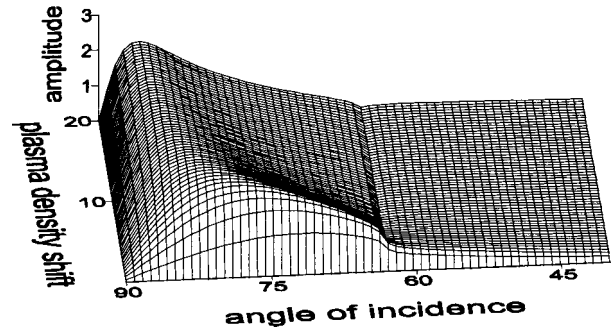


FIG. 6. Amplitude of the forward wave $|B_+|/B_0$ vs the original wave angle of incidence θ_0 and plasma density shift $\Delta N/N_c$ for $\varepsilon_b=10$ and $\varepsilon_1=0.8$ ($\omega_{p1}/\omega_0 \approx 0.96$).

$=90^\circ$ the peak is. It is noteworthy that the height of the peak does not depend on the parameters of the problem such as the initial and final plasma densities or the background dielectric constant. The latter provides similar asymptotic behavior of the surface wave amplitude for gaseous and semiconductor plasmas.

The break of the plot, which corresponds to the total internal reflection angle, moves to the region of smaller angles of incidence with increase of ω_{p1}/ω_0 (or decrease of ε_1), becomes less noticeable, and then disappears at $\omega_{p1}/\omega_0=1$ ($\varepsilon_1=0$) when the plasma for $t<0$ becomes overdense for the original wave. The plot itself does not change significantly and for high density shifts the amplitude is still described by Eq. (18).

The region of total internal reflection, including the most interesting region of the maximum of the amplitude coefficient $|B_+|/B_0$, gets closer to $\theta_0=90^\circ$ with a decrease of the parameter ω_{p1}/ω_0 (i.e., increase of ε_1). It leads to some growth of the maximum value of the amplitude coefficient, which, for example, equals $|B_+|/B_0 \approx 3$ at $\Delta N/N_c \sim 2$ and $\theta_0=87^\circ$ for $\varepsilon_1=0.99$. Then, for $\varepsilon_1=1$ ($\varepsilon_b=10$, $\omega_{p1}/\omega_0 \approx 0.95$) this maximum becomes $|B_+|/B_0 \approx 2$ again and occurs at $\theta_0=90^\circ$. Further decrease of ω_{p1}/ω_0 moves this maximum away from the angle $\theta_0=90^\circ$ (to a few degrees for $\omega_{p1}/\omega_0 \rightarrow 0$) but the maximum value remains approximately the same.

For the case of $\varepsilon_b=1$ the plots $|B_+|/B_0$ are similar to ones for $\varepsilon_b=10$ (under conditions such that the corresponding values of ε_1 are the same) but they exhibit smoother dependence on the plasma density shift $\Delta N/N_c$. For example, when $\varepsilon_b=1$ and $\varepsilon_1=0.8$ ($\omega_{p1}/\omega_0 \approx 0.45$) the most favorable conditions for the forward surface wave excitation regime are achieved at $\Delta N/N_c \sim 15$ (not for $\Delta N/N_c \sim 2$ as shown on Fig. 6).

As for the backward surface wave, its excitation coefficient is much smaller compared to the forward wave for the same values of the incident angle and the density shift; see Fig. 7. In the most interesting region of the effective excitation of the forward wave the amplitude of the backward wave is more than one order of magnitude smaller. A distinguishing feature of Fig. 7 is a sharp peak in $|B_-|/B_0$ in the region of small values of the plasma density shifts $\Delta N/N_c \sim 1$. In general, though, the amplitude coefficient $|B_-|/B_0$ behaves similarly to $|B_+|/B_0$ except that it does not exhibit the maximum near grazing incidence when $\Delta N/N_c \rightarrow \infty$.

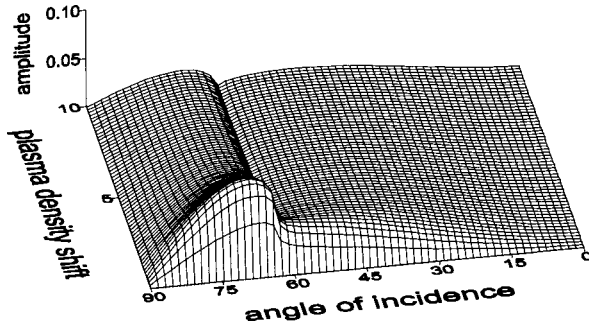


FIG. 7. Amplitude of the backward wave $|B_-|/B_0$ vs the original wave angle of incidence θ_0 and plasma density shift $\Delta N/N_c$ for the same parameters as in Fig. 6.

B. Bulk waves

When $t \rightarrow \infty$ the textbook reflected and transmitted waves due to incidence of wave (1) on a dielectric discontinuity will result. The reflected and transmitted waves of frequency ω_0 are given by the residual contributions of $A_v(s)$, together with the forced response in vacuum, and $A_p(s)$, respectively, at $s = i\omega_0$.

In addition, the wave reflected by the temporal discontinuity of frequency $-\sqrt{\omega_0^2 + \Delta\omega_p^2}$ [forced response in Eq. (13)] impinges from the plasma on the boundary giving rise to two waves of the same frequency: that reflected back into the plasma and that transmitted into vacuum. The amplitudes of the reflected and the transmitted waves are given by the residues of $A_p(s)$ and $A_v(s)$ at $s = -i\sqrt{\omega_0^2 + \Delta\omega_p^2}$ and correspond to the multiplication of the wave incident from the plasma in Eq. (13) by the standard reflection and transmission coefficients [20]. The existence of this component is inherent in the model of a lossless semi-infinite plasma. Moreover, it is not excited if the initial field in the plasma is evanescent ($\varepsilon_1 < \sin^2 \theta_0$) (see Sec. III).

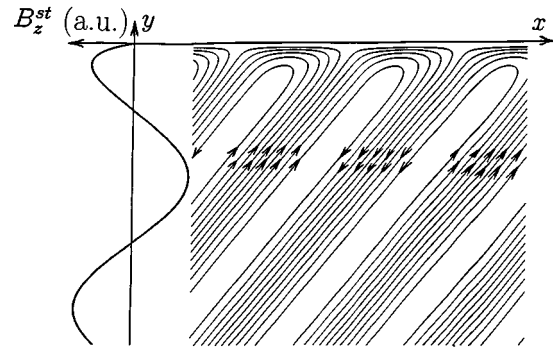
C. Free-streaming mode

This steady-state component of the solution is excited only in the plasma half-space and consists of a static magnetic field and corresponding spatial distribution of dc electric current. Both the time-independent part of the forced response (13) and the residual contribution of $A_p(s)$ at $s = 0$ give the following formula for the magnetic field in the plasma:

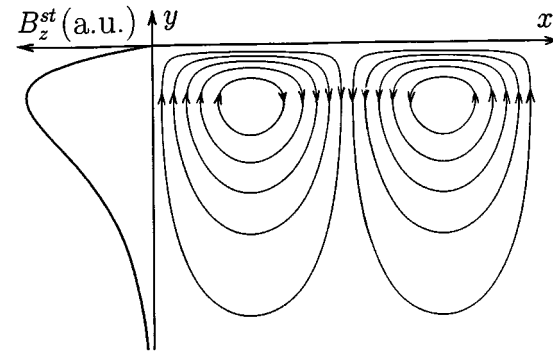
$$B_z^{st}(x, y) = B_0 T \frac{\Delta\omega_p^2 e^{-ih_0 x}}{\omega_0^2 + \Delta\omega_p^2} (e^{ig_1 y} - e^{(\omega_* \sqrt{\varepsilon_b/c}) y}). \quad (19)$$

The second term in Eq. (19) arises due to the change of the constant component of the electron velocity during the transient processes for $t > |y| \sqrt{\varepsilon_b/c}$. The dependence in Eq. (19) has oscillatory character on the y coordinate in the case of an initially transparent plasma medium [see Fig. 8(a)] and a nonoscillatory peaked character in the case of total internal reflection, when $\varepsilon_1 < \sin^2 \theta_0$ [Fig. 8(b)]. The spatial distribution of the dc currents is determined by the magnetic field (19) via Maxwell's equation

$$\mathbf{j}^{st}(x, y) = \frac{c}{4\pi} \text{curl}(\mathbf{B}^{st}) = \frac{c}{4\pi} \left(\hat{\mathbf{x}} \frac{\partial B_z^{st}}{\partial y} + \hat{\mathbf{y}} i h_0 B_z^{st} \right). \quad (20)$$



(a)



(b)

FIG. 8. Structure of the free-streaming mode: qualitative dependence of the static magnetic field B_z^{st} on the y coordinate and the lines of the dc current \mathbf{j}^{st} for (a) $\varepsilon_1 > \sin^2 \theta_0$; (b) $\varepsilon_1 < \sin^2 \theta_0$.

When the original wave undergoes total reflection from the plasma at $t < 0$ the dc current is excited only near the boundary where the initial field was present [see Fig. 8(b)]. The lines of the dc current are similar to the ones in Ref. [25] where the transformation of a surface wave on the boundary of a time-varying plasma was studied. Indeed, the field in the plasma in the case of total reflection is evanescent and has essentially the same features as the surface wave field. When total reflection does not occur at $t < 0$ the dc current lines are parallel to the lines of a constant phase of the initially transmitted wave in the plasma and their intensity varies periodically as the amplitude of the initial wave. Near the boundary these lines are, of course, distorted [Fig. 8(a)].

V. TRANSIENT PROCESSES AND OUTGOING RADIATION

The transient processes are described by the integrals over the branch cuts (see Fig. 2). The outgoing radiation (going from the boundary to $y \rightarrow \pm\infty$) is given by integration over the right sides [$\text{Re}(s) = 0^+$] of the branch cuts in the intervals $\omega_0 \sin \theta_0 < |\omega| < \infty$ for $y > 0$ and $\omega_* < |\omega| < \infty$ for $y < 0$ [$\omega = \text{Im}(s)$]. Evidently, the above mentioned integrals are plane wave expansions of the outgoing radiation. The frequency of a plane wave radiated at an angle θ , which is measured in the (x, y) plane from the normal to the boundary direction both in vacuum and in the plasma ($-\pi/2 < \theta < \pi/2$, $\theta = \pi/2$ coincides with the x direction), follows from the well-known dispersion equations [26] for electromagnetic waves, both in

vacuum and the plasma, and conservation of the x component of the wave vectors

$$\omega = \begin{cases} \frac{\sin \theta_0}{\sin \theta} \omega_0, & \text{if } y > 0 \\ \frac{\omega_*}{\sin \theta} \sqrt{1 - \frac{\omega_{p2}^2}{\omega_*^2} \cos^2 \theta}, & \text{if } y < 0. \end{cases} \quad (21)$$

Negative frequencies correspond to the waves radiated backwards under angles $\theta < 0$. The waves of the lowest frequencies ($\pm \omega_0 \sin \theta_0$ in vacuum and $\pm \omega_*$ in the plasma) travel along the boundary ($\theta = \pm \pi/2$). Higher frequency waves are radiated under smaller angles—up to $|\omega| \rightarrow \infty$ for $\theta \rightarrow 0$.

Follow the technique proposed in Ref. [27] we calculate the radiation field energy (per unit area of the plasma-vacuum interface) in vacuum (W_v) and in the plasma (W_p) asymptotically when $t \rightarrow \infty$ by integration over y energy density which can be expressed in terms of the above mentioned integrals. The result can be written as

$$W_{v,p} = \int_{-\pi/2}^{\pi/2} W_{v,p}(\theta) d\theta, \quad (22)$$

where the angular density of radiation energy $W_{v,p}(\theta)$ is

$$W_{v,p}(\theta) = \frac{c \omega_0 \sin \theta_0}{16 \pi^2 (\varepsilon_b)_p} \cot^2 \theta |A_{v,p}(s = i\omega)|^2, \quad (23)$$

with $(\varepsilon_b)_p$ implied to be taken only for W_p and $\omega(\theta)$ given by (21). Certainly, the same result may be obtained also by integrating over time the electromagnetic energy flux through a unit area parallel to the boundary. The signs of the double-valued functions $\kappa_{v,p}$ in $A_{v,p}$ should be taken to satisfy the requirement that the corresponding waves travel away from the boundary or are evanescent, i.e., the imaginary part of $\kappa_{v,p}$ has the same sign as the angle θ or its real part is positive. The latter case occurs for angles greater than the total internal reflection angle. In the case of total reflection from the plasma, $\kappa_p(s = i\omega) = \sqrt{\varepsilon_b(\omega_*^2 - \omega^2)}/c$ is real in A_v if $\omega_* > \omega_0 \sin \theta_0$ for $\tilde{\theta}_v < |\theta| < \pi/2$, $\sin \tilde{\theta}_v = (\omega_0/\omega_*) \sin \theta_0$. For total reflection from vacuum, which is only possible for $\varepsilon_b > 1$, $\kappa_v(s = i\omega) = \sqrt{\omega_0^2 \sin^2 \theta_0 - \omega^2}$ is real in A_p if $\omega_* < \omega_0 \sin \theta_0$ for $\tilde{\theta}_p < |\theta| < \pi/2$, $\sin \tilde{\theta}_p = \omega_0 \sin \theta_0 / \sqrt{\varepsilon_b(\omega_0^2 \sin^2 \theta_0 - \omega_p^2)}$. The condition $\omega_* < \omega_0 \sin \theta_0$ reduces easily to the inequality $N_2/N_c < (\sin^2 \theta_0)(1 - \varepsilon_b^{-1})$.

Figures 9(a) and 9(b) show the angular distribution of the energy radiated into vacuum and into the plasma. The infinite peaks of the angular densities $W_{v,p}(\theta)$ corresponding to the frequencies ω_0 and $\pm \sqrt{\omega_0^2 + \Delta \omega_p^2}$ are a peculiarity of our assumption of an incident plane wave of infinite extent and the lossless semi-infinite plasma. This artifact is also related to the formation process of the steady-state pattern of bulk waves described in Sec. IV B. Obviously, the waves with $\omega \approx \omega_0$ represent the radiation of the old ($t < 0$) reflected wave in vacuum and the formation of the new reflected and transmitted waves in vacuum and the plasma, respectively. The corresponding angles are θ_0 in vacuum and $\sin \theta = \sin \theta_0 / \sqrt{\varepsilon_2(\omega_0)}$ in the plasma. If $\varepsilon_2(\omega_0) < \sin^2 \theta_0$, i.e.,

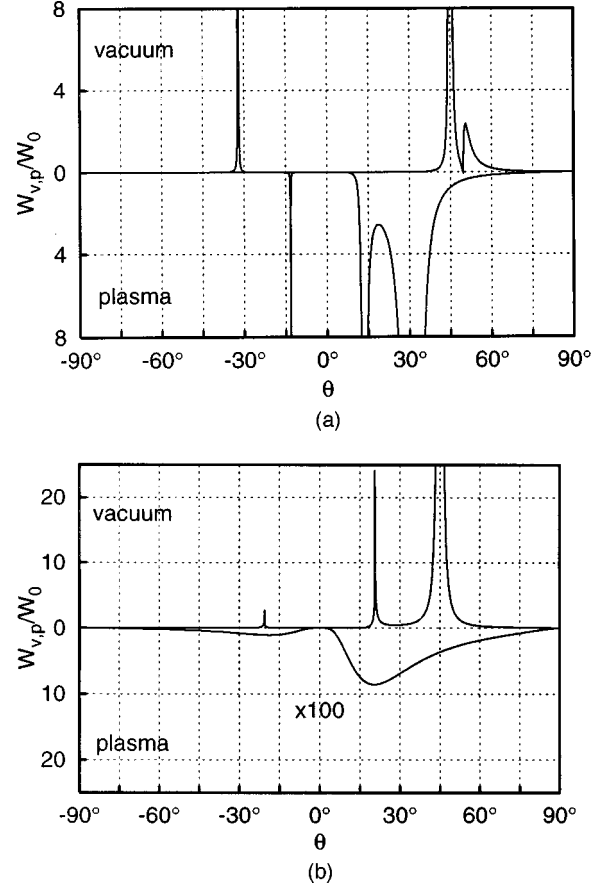


FIG. 9. Angular densities of the transient radiated energy $W_{v,p}(\theta)$ (normalized to the quantity $W_0 = B_0^2 c / 4 \omega_0$, which is the energy of the original wave incident normally on a unit area of the boundary per period of the wave) vs the angle of radiation θ for (a) $\varepsilon_b = 10$, $\theta_0 = 45^\circ$, $\omega_{p1}/\omega_0 = 0.2$, $\omega_{p2}/\omega_0 = 0.9$ [$\varepsilon_1 > \sin^2 \theta_0$ and $\varepsilon_2(\omega_0) > \sin^2 \theta_0$]. The spectrum in vacuum is dominated by the infinite peaks near ω_0 at $\theta \approx 45^\circ$ and $-\sqrt{\omega_0^2 + \Delta \omega_p^2}$ at $\theta \approx -32^\circ$. The finite peak at frequency ω_* is at $\theta \approx 50^\circ$. In the plasma there are infinite peaks at frequencies ω_0 ($\theta \approx 31^\circ$) and $\pm \sqrt{\omega_0^2 + \Delta \omega_p^2}$ ($\theta \approx \pm 13^\circ$). (b) $\varepsilon_b = 10$, $\theta_0 = 45^\circ$, $\omega_{p1}/\omega_0 = 1.1$, $\omega_{p2}/\omega_0 = 2$ ($\varepsilon_1 < \sin^2 \theta_0$). The spectrum in vacuum is dominated by the infinite peak at frequency ω_0 ($\theta \approx 45^\circ$). The finite peaks of frequency $\pm \omega_*$ are near $\theta \approx \pm 21^\circ$. In the plasma there are no clearly shaped peaks, the radiation has relatively broad spectrum and low intensity (its magnitude was multiplied by the indicated scale factor).

plasma is not transparent for the incident wave after the shift, the peak of W_p at $\omega = \omega_0$ is absent [Fig. 9(b)]. The radiation of frequencies $\omega \approx \pm \sqrt{\omega_0^2 + \Delta \omega_p^2}$ is created by the evolution of the forced waves in the plasma [the second term in Eq. (13)] at $t > 0$. The corresponding peaks lie at the angles given by $\sin \theta = \pm \sin \theta_0 / \sqrt{\varepsilon_1}$ in the plasma and $\sin \theta = -\omega_0 \sin \theta_0 / \sqrt{\omega_0^2 + \Delta \omega_p^2}$ in vacuum [Fig. 9(a)]. It is noteworthy that the forced wave traveling towards the boundary in the plasma (with frequency $-\sqrt{\omega_0^2 + \Delta \omega_p^2}$) always gives rise to radiation into vacuum, i.e., it cannot undergo total reflection from the boundary. If $\varepsilon_1 < \sin^2 \theta_0$, i.e., the original wave undergoes total internal reflection at $t < 0$, the peaks in the plasma are absent (in this case $\sqrt{\omega_0^2 + \Delta \omega_p^2} < \omega_*$ whereas radiation into the plasma has $|\omega| > \omega_*$) while in vacuum there is a strong peak at ω_* and a relatively small

one at $-\omega_*$. In general, the finite bursts of radiation at the frequencies $\pm \max\{\omega_0 \sin \theta_0, \omega_*\}$ correspond to the critical angle of total internal reflection from vacuum if $\omega_0 \sin \theta_0 > \omega_*$ or from plasma if $\omega_0 \sin \theta_0 < \omega_*$. The shape of these peaks is essentially asymmetrical; it falls off slowly at lower frequencies and fast for higher frequencies. If $\omega_* < \omega_0 \sin \theta_0$ (possible only for $\epsilon_b > 1$) these peaks are located in the plasma at the frequencies close to $\pm \omega_0 \sin \theta_0$ [this case is not presented in Figs. 9(a) and 9(b)]. If $\omega_* > \omega_0 \sin \theta_0$ the peaks move to vacuum and occur at $\pm \omega_*$ [see Figs. 9(a) and 9(b), the peak at $-\omega_*$ is too small in Fig. 9(a)]. Moreover, if $\omega_* > \sqrt{\omega_0^2 + \Delta\omega_p^2}$, which corresponds to the total internal reflection of the original wave at $t < 0$ ($\epsilon_1 < \sin \theta_0$), the maximum frequency of radiation in vacuum is $\pm \omega_*$ and these peaks become strongly enhanced while the peaks at $\pm \sqrt{\omega_0^2 + \Delta\omega_p^2}$ in the plasma and $-\sqrt{\omega_0^2 + \Delta\omega_p^2}$ in vacuum disappear as we pointed out above. Evidently, the strong enhancement of the peaks at $\pm \omega_*$ in the case of total reflection of the original wave can be explained by the radiation of the energy initially present in the plasma to vacuum at frequencies $\pm \omega_*$. Consequently, the magnitude of these peaks decreases with ω_{p1} since the penetration depth of the original wave into the plasma becomes smaller. It is important to emphasize that due to the fast rolloff of the angular densities $W_{v,p}$ for $|\omega(\theta)| > \max\{\omega_*, \sqrt{\omega_0^2 + \Delta\omega_p^2}\}$ [Figs. 9(a) and 9(b)] these frequencies put an upper limit on the frequency of the generated waves. Also it is essential that for $\omega_* > \sqrt{\omega_0^2 + \Delta\omega_p^2}$ the maximum frequency shift (ω_*) surpasses the one for the case of the plasma density shift in the entire space ($\sqrt{\omega_0^2 + \Delta\omega_p^2}$) [6,7], which yields more efficient frequency upshift. We point out again that besides being frequency upshifted, the radiation is angularly resolved, which provides an extra advantage of the bounded plasma over unbounded in creation of tunable sources of radiation.

VI. CONCLUSION

To conclude, we have presented the theory of interaction of a plane electromagnetic wave with a nonstationary plasma half-space when its density instantaneously grows in time for the general case of oblique incidence and TM polarization of the wave. The emphasis has been made on the investigation of the qualitatively new phenomenon of the creation of two frequency downshifted surface waves propagating in the opposite directions along the plasma boundary. We have given the complete picture of the excited steady-state modes and described the transient processes for the case of gaseous and solid-state plasmas.

Although we have analyzed the evolution of an incident plane wave the results of our study can be straightforwardly generalized for the case of incident beams of a finite (but

relatively large compared to the wavelength) width. In this case the surface waves that are created are quasimonochromatic wave packets whose length is defined by the area covered by the incident beam. The assumption of a uniform ionization of the entire plasma half-space can also be weakened in the case of total internal reflection of the original wave; it is sufficient to assume that the depth of the uniform ionization is larger than that of the penetration of the original wave into the plasma and the degree of ionization decreases gradually with the distance from the plasma boundary, which actually occurs in the case of ionization by controlling irradiation from vacuum into the plasma.

The phenomenon of trapping described above may be verified experimentally with an experimental setup similar to the one described in Ref. [10] where a transient plasma was created on a time scale < 1 ns via electric discharge between the plates of a plane capacitor in a vacuum chamber filled with a gas. If we illuminate the emerging plasma slab from the side by a beam of cm-wavelength radiation the trapped surface wave should be detected at the far end of the slab. The phenomenon of trapping pointed out here in the parametric approach may be realized as a nonlinear effect when two superstrong microwave beams cross and produce plasma [28]; a part of the beams' electromagnetic energy should be trapped by the plasma slabs that are generated. This phenomenon may be essential in the formation stretched plasma structures similar to observed in Ref. [29].

However, the most significant application of the phenomenon is the creation of entirely new components for input of electromagnetic radiation into planar waveguiding structures with solid-state plasma (semiconductor) slabs. The nonstationarity of the semiconductor medium may be provided by a number of different mechanisms, e.g., carrier injection [30], photoionization by a laser pulse [14,15], effective mass switching [31], etc. The typical time for plasma creation in those cases lies within the picosecond range; these mechanisms can be used for transient input of millimeter and submillimeter radiation. The simplest scheme includes a semiconductor slab waveguide where the carrier density grows rapidly in time due to effect of a laser pulse; the signal wave is trapped by the slab as a result [32]. Finally, another possible scheme is when the slab waveguide is stationary (e.g., dielectric) but coated with a plasma film with controlled carrier density [33].

ACKNOWLEDGMENTS

One of us (M.I.B.) was supported in part by the Russian Ministry of Education under Grant No. 95-0-8.2-33. A critical reading of the manuscript by D. S. Citrin is gratefully acknowledged.

-
- [1] R. L. Fante, IEEE Trans. Antennas Propag. **19**, 417 (1971).
 [2] D. K. Kalluri, IEEE Trans. Plasma Sci. **16**, 11 (1988).
 [3] D. K. Kalluri and V. R. Goteti, J. Appl. Phys. **72**, 4575 (1992).
 [4] D. K. Kalluri, IEEE Trans. Plasma Sci. **21**, 77 (1993).
 [5] M. I. Bakunov and S. I. Zaitsev (unpublished).

- [6] C. L. Jiang, IEEE Trans. Antennas Propag. **23**, 83 (1975).
 [7] S. C. Wilks, J. M. Dawson, and W. B. Mori, Phys. Rev. Lett. **61**, 337 (1988).
 [8] V. I. Semenova, Sov. Radiophys. Quantum Electron. **10**, 599 (1967).

- [9] R. L. Savage, Jr., R. P. Brogle, W. B. Mori, and C. Joshi, *IEEE Trans. Plasma Sci.* **21**, 5 (1993).
- [10] S. P. Kuo and A. Ren, *IEEE Trans. Plasma Sci.* **21**, 53 (1993).
- [11] C. J. Joshi, C. E. Clayton, K. Marsh, D. B. Hopkins, A. Sessler, and D. Whittum, *IEEE Trans. Plasma Sci.* **18**, 814 (1990).
- [12] C. H. Lai, R. Liou, T. C. Katsouleas, P. Muggli, R. Brogle, C. Joshi, and W. B. Mori, *Phys. Rev. Lett.* **77**, 4764 (1996).
- [13] X. Xu, N. Yugami, and Y. Nishida, *Phys. Rev. E* **55**, 3328 (1996).
- [14] K. H. Schoenbach, V. K. Lakdawala, R. Germer, and S. T. Ko, *J. Appl. Phys.* **63**, 2460 (1988).
- [15] A. Kost, L. West, T. C. Hasenberg, J. O. White, M. Matloubian, and G. C. Valley, *Appl. Phys. Lett.* **63**, 3494 (1993).
- [16] *Surface Polaritons*, edited by V. M. Agranovich and D. L. Mills (North-Holland, New York, 1982).
- [17] *Electromagnetic Surface Modes*, edited by A. D. Boardman (Wiley, New York, 1982).
- [18] F. DeMartini and Y. R. Shen, *Phys. Rev. Lett.* **36**, 216 (1976).
- [19] M. I. Bakunov and A. V. Maslov, *J. Commun. Technol. Electron.* (to be published).
- [20] L. D. Landau and E. M. Lifshitz, *Electrodynamics of Continuous Media* (Pergamon Press, Oxford, 1960).
- [21] C. H. Lai, T. C. Katsouleas, W. B. Mori, and D. Whittum, *IEEE Trans. Plasma Sci.* **21**, 45 (1993).
- [22] This assumption is valid even if the new born electrons have nonzero velocities but distributed isotropically. See, e.g., V. B. Gildenburg, A. V. Kim, V. A. Krupnov, V. E. Semenov, A. M. Sergeev, and N. A. Zharova, *IEEE Trans. Plasma Sci.* **21**, 34 (1993).
- [23] *Handbook of Surfaces and Interfaces, Vol. 3, Surface Phonons and Polaritons*, edited by A. A. Maradudin, R. F. Wallis, and L. Dobrzynski (Garland, New York, 1980).
- [24] C. M. Krowne, *IEE Proc. H* **140**, 147 (1993).
- [25] M. I. Bakunov and S. N. Zhukov, *Plasma Phys. Rep.* **22**, 649 (1996).
- [26] V. L. Ginzburg, *The Propagation of Electromagnetic Waves in Plasmas* (Pergamon, Oxford, 1970).
- [27] V. L. Ginzburg and V. N. Tsytovich, *Transition Radiation and Transition Scattering* (Hilger, Bristol, 1990).
- [28] S. P. Kuo, *Phys. Rev. Lett.* **65**, 1000 (1990).
- [29] A. Sola, J. Cotrino, A. Gamero, and V. Colomer, *J. Phys. D* **20**, 1250 (1987).
- [30] O. Mikami and H. Nakagome, *Electron. Lett.* **20**, 228 (1984).
- [31] M. Kuijk and R. Vounckx, *Electron. Lett.* **25**, 231 (1989).
- [32] M. I. Bakunov and A. V. Maslov, *Phys. Rev. Lett.* **79**, 4585 (1997).
- [33] M. I. Bakunov and A. V. Maslov, *J. Appl. Phys.* **83**, 3885 (1998).